Hindawi
Journal of Food Processing and Preservation
Volume 2023, Article ID 9994657, 12 pages
https://doi.org/10.1155/2023/9994657

Research Article

Characterization of Cocoa Butter Replacer Developed from Agricultural Waste of Mango Kernel and Rice Bran

Mansura Mokbul, Yuen Lin Cheow, and Lee Fong Siow

School of Science, Monash University Malaysia, 47500 Bandar Sunway, Selangor, Malaysia

Correspondence should be addressed to Lee Fong Siow; siow.lee.fong@monash.edu

Received 23 July 2023; Revised 27 November 2023; Accepted 7 December 2023; Published 23 December 2023

Academic Editor: Fabiano A.N. Fernandes

The unique physicochemical properties of cocoa butter (CB) provide the desired physical properties in chocolate. Due to its high demand, increasing price, and limited supply, people are looking for cocoa butter alternatives (CBAs). In this study, CBA was prepared using enzymatic acidolysis on mango kernel fat stearin with rice bran oil blend. Reaction parameters (time (4-8 h), temperature (50-70°C), and enzyme load (6-10%, *w*/*w*)) were optimized using response surface methodology to produce similar triacylglycerol (TAG) composition as CB, and the properties of different proportions of CBAs with CB were assessed. Triacylglycerol content, melting behavior, solid fat content, crystal morphology, and polymorphism were investigated by high-performance liquid chromatography, differential scanning calorimetry, pulse nuclear magnetic resonance, polarized light microscopy, and X-ray diffraction, respectively. The optimum reaction condition to produce comparable percentages of monounsaturated TAGs in the final product was 8 h time, 8% enzyme load, and 50°C. After blending of CBA with CB in different proportions, no significant differences in terms of polymorphism, melting profile, and solid fat content were observed up to 20% CBA replacement. However, the TAG profile was similar up to 10% replacement of CB with CBA. In summary, the enzymatically produced CBA can potentially be used as a cocoa butter replacer up to 20% in the confectionery industry.

1. Introduction

Cocoa butter (CB) is the main component of chocolate or chocolate-related substances. CB is extracted from *Theobroma cacao* seeds and represents the continuous phase of chocolate which combines the other nonfat ingredients (sugar, cocoa powder, etc.) in it [1]. CB is popular because of its unique chemical and physical (melting, rheology, and crystallization) characteristics. This unique profile gives a specific snap, gloss, and textural profile, which is a desirable property in food industries [2]. Its distinctive triacylglycerol (TAG) composition is the foundation of these remarkable physical characteristics. The major portion of total TAGs mainly consisted of POP, StOSt, and POSt (P, palmitic; O, oleic; and St, stearic acid) [3, 4]. CB can form different polymorphs such as α, $\beta'1$, $\beta'2$, $\beta1$, and $\beta2$ [2]. The preferable polymorph for chocolate is $\beta2$ as its melting temperature ranges from 32 to 34°C [2].

Due to its high demand and low supply, there is increasing interest in cocoa butter alternatives (CBAs). Among CBAs, cocoa butter equivalents (CBEs) and cocoa butter replacers (CBRs) are produced from non-lauric-based fats. Cocoa butter substitutes (CBSs) are usually obtained from lauric-based fats [5]. Mango kernel fat (MKF) is rich in stearic acid (24-57%) [6], which leads to higher content of StOSt (29.99–55.44%) [7]. The StOSt range is wide as it is influenced by mango origin, variety, and maturation. Kochhar [8] reported that mango kernel fraction, which contains 59% of StOSt, can be used as a CBE. There were few works reported on blending of various fats to prepare CBAs. Jahurul et al. [9] prepared CBR by blending MKF with palm stearin; Biswas et al. [2] blended palm kernel oil (PKO) and

bleached and deodorized PKO and palm midfraction (PMF) to produce CBSs, and Sonwai et al. [5] prepared CBEs from PMF and MKF blends.

Oil can be modified using different techniques based on their final desired outcomes. Fractionation is a widely used technique that helps to separate solid and liquid portions of a fat based on their crystallization points [10]. Enzymatic interesterification and chemical interesterification are two techniques used to modify the lipid structures where chemical processing is less expensive with more advantages [11, 12]. To have similar saturate-unsaturate-saturate TAG composition as CB, different oil blends were treated with lipase enzyme to perform acyl incorporation or acyl migration [13, 14]. The quantity of desired fatty acid (FA) (donor) integrated into sn-1,3 places (sn-1,3 incorporation) or sn-1,2,3 positions is referred to as acyl incorporation. Acyl migration is defined as the amount of desired FA (donor) that migrated into the sn-2 location [12]. Depending on the desired output product, the acyl donor and lipozyme enzymes are varied [14, 15]. FA residues in the sn-2 position are not altered by the incorporation of fatty acids into the sn-1,3 positions by 1,3-specific lipase [16]. Position-specific lipozyme enzymes help to alter FA in glycerol backbone in a controlled manner. Previously, different sn-1,3 position-specific lipozyme enzymes, such as Lipozyme TL IM or Lipozyme RM IM, were used in various studies to alter FA positions along the glycerol backbone [11, 13, 17]. With the advantages of less energy usage, no isomerization by-products, and greater final product control, this aids in producing the desired TAGs after modification [16]. To prepare CBA, the desired TAG profile is to mimic TAG profile of CB. CB contains about 15.6% POP, 45.5% POSt, and 27.6% StOSt (P, palmitic acid; O, oleic acid; and St, stearic acid) [13].

Previously, palm oil with stearic and palmitic acid mixture [15], palm oil midfraction with hardened soybean oil [18], tea seed oil with palmitate and stearate mixture [14], and sunflower oil with the mixture of palmitic, stearic, myristic, and arachidic acids [11] were used to produce CBAs in the presence of various lipozyme enzymes. Different variables in the acidolysis reaction, such as time, temperature, enzyme load, water content, and substrate-enzyme ratio, impacted greatly on the reaction output [15]. These conditions are needed to be optimized to produce different CBAs. Response surface methodology (RSM) is a popular technique which has been used in various studies to optimize different factors by using mathematical and statistical analyses for the desired final product [19].

MKF consists of high stearic acid although the level varies based on mango variety, maturity, and origin [6]. While the StOSt content varies considerably based on a number of variables, fractionation may be used to improve the content of stearic acid, hence improving the StOSt profile of MKF. The stearic acid content and StOSt content of MKF can be further improved using the fractionation process. In contrast, rice bran oil (RBO) is rich in oleic and palmitic acids; it also contains various bioactive compounds like phenolic acids, anthocyanins, and flavonoids [20–22]. Along with a high stearate level, MKF contains antioxidant value which is closer to CB. These bioactive compounds and antioxidant properties are beneficial for health [23]. Mango and rice production are rising annually worldwide [24]. Mango seed and rice bran are the by-products or waste. Proper management and reuse of these by-products is sustainable and beneficial for the environment and economy. Blending MKF-stearin fraction with RBO will help to improve the FA content as CB. To mimic TAG composition of CB, alteration of glyceride backbone is needed by acidolysis reaction. Reaction condition optimization is necessary to produce the desired level of modification to produce CBA. It is also necessary to assess the physicochemical properties of the final product, which gives the opportunity to decide the possible replacement percentages with CB. This study is aimed at optimizing the acidolysis reaction condition using RSM followed by characterization of the physicochemical properties of the CBA in various proportions with CB.

2. Materials and Methods

2.1. Materials. Samples of MKF and RBO were purchased from Personal Formula Resources in Malaysia and a local store in Malaysia, respectively. The FA and TAG standards were obtained from Sigma-Aldrich, Germany. Acetone, ethanol, *n*-hexane, and anhydrous methanol were purchased from Fisher, Malaysia. All these chemicals were analytical or high-performance liquid chromatography (HPLC) grade. Le Bourne Sdn Bhd (Malaysia) was the supplier of CB.

2.2. Fractionation. Solvent fractionation was carried out to separate the liquid portion and solid crystals from one another. This method was adopted from Jin et al. [25] with some modifications. MKF was melted completely at 80°C, mixed with acetone in a 1 : 5 (oil/acetone) ratio, and kept for 100 min at 13°C. The ratio of 1 : 5 between oil and acetone was selected based on preliminary experiments conducted to achieve optimal separation efficiency. Then, it was filtered by vacuum filtration. The solid stearin portion was separated from the liquid olein part. Then, a rotavapor (Eyela, OSB-2100, Shanghai, China) was used to remove the rest of the solvent from the stearin portion. Finally, the sample was kept in a fume hood to allow trace amounts of solvent to evaporate before storing in a refrigerator.

2.3. Preparation of Oil Blends. MKF-stearin fraction and RBO oil were combined in 11 different mass ratios. MKF-stearin fraction and RBO were melted completely in the oven at 70°C and 40°C, respectively. Subsequently, these were blended as MKF-stearin/RBO in the following mass ratios: A (0 : 100), B (10 : 90), C (20 : 80), D (30 : 70), E (40 : 60), F (50 : 50), G (60 : 40), H (70 : 30), I (80 : 20), J (90 : 10), and K (100 : 0). As a benchmark comparison, CB was used.

2.4. Fatty Acid Analysis. The FA profile of the fat blends was analyzed by gas chromatography (GC) using fatty acid methyl ester with flame-ionized detector. A GC (PerkinElmer Clarus 500 GC, USA) fitted with an elite FFAP column (30 m length × 0.32 mm interior diameter × 0.25 μm film thickness) was used. In a 2 mL vial, 50 mg of sample was

added with 0.95 mL of *n*-hexane, and 0.05 mL of 1 M sodium methoxide in anhydrous methanol was mixed in the vial and shaken vigorously for 6-7 s in a vortex mixture. After the sedimentation, 1 μL of the clear supernatant was injected into a GC for analysis. The injection and detection temperatures were both at 250°C. The oven temperature was programmed as follows: heated from 110 to 140°C (30°C/min), hold at 140°C for 1 min, heated from 140 to 240°C (15°C/min), and hold for 7 min at 240°C. Helium was used as the carrier gas with a flow rate of 0.9 mL/min [17]. Fatty acid methyl ester standard retention time was used to identify individual FA. A peak area normalization method was used to quantify the FAs.

2.5. Acidolysis Reaction. Acidolysis reaction was performed with oil blends and palmitic acid in the presence of Lipase TL-IM enzyme (Novozymes). Oil blend (MKF-stearin/RBO, 50 : 50) and 10% palmitic acid were mixed together and heated up to melt. MKF-stearin/RBO oil blend was selected based on their FA composition, and 10% palmitic acid was added to ensure the presence of sufficient palmitic acid during the acidolysis reaction. Acidolysis reaction was performed at different temperature, time, and enzyme load combination with a 250 rpm rotation speed [17]. The reaction was started with the addition of enzyme into the oil blends and ended by filtering the enzyme using a double-layer cheese cloth filter.

2.6. Experimental Design. To optimize the design condition, a central composite design (CCD) model was applied. Time (4-8 h), reaction temperature (50-70°C), and enzyme load (4-8%, *w*/*w*) were selected to achieve the optimum level of saturate–oleoyl–saturate (SOS; POP, StOSt, and POSt where P is the palmitic acid, O is the oleic acid, and St is the stearic acid) combination of TAGs. A total of 20 runs were performed with duplicates. Table 1 represents the variables with their ranges. The total SOS percentages were employed as the output factor to optimize the reaction condition for acidolysis reaction. A detailed table of factor variables and observed and predicted values is shown in Table S1.

2.7. Free Fatty Acid (FFA) Removal and Preparation of CB and CBA Blends. A mixture of 10 mL oil (final product after acidolysis of 50 : 50 oil blend with 10% palmitic acid) with 1 mL of 20% NaOH solution was stirred at 800 rpm. To break up any emulsion, this mixture was heated at 70°C for 25 min followed by immediate centrifugation at 40°C and 4000 rpm for 20 min to remove the soap [17]. FFA was determined by using American Oil Chemists' Society (AOCS) Official Method Ca 5a-40, as percentage of stearic acid. Then, the produced CBA was blended with CB at different percentages of 5%, 10%, 20%, 30%, 40%, and 50% as a replacement with CB.

2.8. Triacylglycerol (TAG) Analysis. TAG was determined using the high-performance liquid chromatography (HPLC) using ZORBAX C-18 column (4.6 × 250 mm, 5 mm, Agilent Technologies, CA, USA, Agilent, CA, USA). Column oven temperature and pressure were maintained at 35°C and 6-7 MPa, respectively, and isocratic elution was carried out at a rate of 1 mL/min. For the analysis, the method established by American Oil Chemists' Society (Ce 5b-89) was followed. Acetone and acetonitrile (70 : 30, *v*/*v*) were used as mobile phase, and a refractive index detector (RID 1260 Infinity; CA, USA) was used. Oil was dissolved in acetone (5% (*w*/*v*)), and 10 μL of oil dissolved in acetone was injected into HPLC using an autoinjector. The retention time of TAG standards was used as a reference to identify the respective TAGs. Peak area was used for percentage area calculation.

Table 1: Experimental values and range for independent variables for acidolysis reaction.

Variable identity	Variable (unit)	Level		
		-1	0	1
A	Time (h)	4	6	8
B	Temperature (°C)	50	60	70
C	Enzyme load (%)	4	6	8

2.9. Melting Profile Analysis. Melting profile was analyzed using differential scanning calorimetry (DSC; Pyris 4000 DSC; PerkinElmer, USA). About 5 to 10 mg oil was sealed in an aluminum pan. The reference pan was empty, and nitrogen gas flow rate was 20 mL/min. Initially, samples were cooled at -50°C and then heated with a heating rate of 5°C/min up to 80°C. The melting curve was recorded from -50°C to 80°C.

2.10. Solid Fat Content (SFC) Analysis. Pulse nuclear magnetic resonance (p-NMR) with a Bruker Minispec PC 120 NMR analyzer (Karlsruhe, Germany) was used to determine SFC of the blends and CB. AOCS Official Method Cd 16b-93 was used for SFC analysis. Samples were melted completely at 100°C for 15 min. Then, 2 to 3 g of samples was filled into NMR tubes (10 mm outside diameter × 75 mm length, up to 3 cm in height). Samples were tempered at 60°C for 5 min, followed by 0°C for 90 min, 26°C for 40 h, and 0°C for 90 min, and finally kept for 60 min at the desired measuring temperatures from 5 to 65°C. Finally, SFC were measured between temperatures 5 and 65°C with 5°C intervals.

2.11. Polymorphism Analysis. A D8 Discover X-ray diffractometer fitted with Cu-Kα radiation ($k = 1.5418$ Å, voltage 40 kV, and current 40 mA) was used to analyze polymorphism of fat blends and CB. Samples were stored at 24°C for 24 h before analysis for proper crystal growth. At room temperature, the samples were assessed with a scan rate of 1.5°/min at 2θ angles of 10° to 30° [17]. The EVA-diffraction software (Bruker, Germany) was used to determine short (d) spacing (Å). Assignments of polymorphs were based on the following short spacing characteristics of CB: α form ($d = 4.15$ Å), β' forms ($d = 3.8 - 4.3$ Å), and β forms ($d = 4.5 - 4.6$ Å) [2].

2.12. Crystal Morphology Analysis. Crystal microstructures were analyzed using polarized light microscopy (PLM, Olympus BX51, Tokyo, Japan). A digital camera (Nikon, DS-Filc, Tokyo, Japan) and NIS-Elements Imaging Software (version 4.20) were equipped with a microscope, and crystal

Table 2: FA profile (peak area %) of CB, MKF-stearin, and RBO blends.

Blends	Fatty acids				
	C14	C16	C18	C18:1	C18:2
CB	0.04 ± 0.04^{h}	27.7 ± 0.93^{a}	36.39 ± 0.65^{e}	33.13 ± 0.28^{e}	2.73 ± 0.03^{k}
A (0 : 100)	0.41 ± 0.03^{a}	21.05 ± 0.41^{b}	1.73 ± 1.08^{k}	42.87 ± 0.72^{a}	33.85 ± 0.46^{a}
B (10 : 90)	0.41 ± 0.03^{a}	20.39 ± 0.50^{b}	8.78 ± 0.21^{j}	40.16 ± 0.28^{b}	30.24 ± 0.11^{b}
C (20 : 80)	0.38 ± 0.02^{ab}	19.81 ± 0.57^{bc}	14.35 ± 0.21^{i}	38.03 ± 0.25^{c}	27.43 ± 0.17^{c}
D (30 : 70)	0.32 ± 0.01^{bc}	19.02 ± 0.52^{bc}	20.29 ± 0.24^{h}	35.4 ± 0.23^{d}	24.35 ± 0.09^{d}
E (40 : 60)	0.29 ± 0.03^{cd}	18.77 ± 1.02^{bc}	26.25 ± 0.58^{g}	33.49 ± 0.32^{e}	21.13 ± 0.15^{e}
F (50 : 50)	0.24 ± 0.01^{cde}	17.67 ± 0.43^{cd}	32.90 ± 0.12^{f}	31.26 ± 0.24^{f}	17.69 ± 0.63^{f}
G (60 : 40)	0.23 ± 0.05^{de}	17.80 ± 1.49^{cd}	38.23 ± 1.18^{e}	28.85 ± 0.37^{g}	14.85 ± 0.09^{g}
H (70 : 30)	0.17 ± 0.02^{ef}	16.2 ± 1.54^{de}	45.01 ± 1.03^{d}	26.93 ± 0.48^{h}	11.70 ± 0.17^{h}
I (80 : 20)	0.14 ± 0.01^{fg}	15.94 ± 0.49^{de}	49.82 ± 0.57^{c}	25.35 ± 0.13^{i}	8.73 ± 0.03^{i}
J (90 : 10)	0.08 ± 0.01^{gh}	15.23 ± 0.24^{e}	56.88 ± 0.28^{b}	22.34 ± 0.32^{j}	5.46 ± 0.06^{j}
K (100 : 0)	0.01 ± 0.0^{h}	15.71 ± 0.71^{de}	58.57 ± 0.55^{a}	22.12 ± 0.31^{j}	2.58 ± 0.12^{k}

[1]Each value represents mean ± standard deviation of the three replicates ($n = 3$). Different superscript letters in the same column represent significant statistical differences ($p < 0.05$). [2]CB = cocoa butter; RBO = rice bran oil; MKF-stearin = mango kernel fat-stearin; CBA = cocoa butter alternative; P = palmitic acid; O = oleic acid; St = stearic acid.

network was observed at 24°C for all the sample blends and CB. The method details were adopted and modified from Narine and Marangoni [26]. The melted sample (about 15 μL) was placed on a glass slide and covered with a coverslip. To ensure crystallization, samples were kept at 24 ± 1°C for 48 h. Crystal portions appeared as grey or white whereas black region indicated liquid phase.

2.13. Statistical Analysis. RSM was applied to optimize the reaction condition by Design-Expert 13. To assess the significance of the differences among the samples, a one-way ANOVA with a 95% significance level with a Tukey post hoc test was carried out using the Statistical Package for the Social Sciences (SPSS). All analyses were performed in triplicate and reported as mean with standard deviation, with the exception of the SFC analysis, which was conducted in duplicate.

3. Results and Discussion

3.1. Fractionation of MKF. Fractionation is an effective and approved fat processing technique by the European Union (Directive 2000/36/EC) [27]. Fractionation helps to separate liquid olein and solid stearin fractions depending on their crystallization profiles. Table 2 demonstrates the yield percentages of fractionated MKF.

Yields of 64.5 ± 1.2% and 35.5 ± 1.4% were recorded for stearin and olein fractions of MKF, respectively, after 100 minutes of fractionation with acetone. These values are comparable with a previous study by Jin et al. [7] who reported a 57.9% yield of first stearin fraction. Fat yields may vary (5.65-11.14%) with mango variety, origin, and maturity. Due to multistage fractionation, the yields of stearin (52.8-57.9%) and olein (23.6-40.6%) fraction also differ [7]. The stearin fraction with higher melting profile is used in the subsequent study.

3.2. Fatty Acid Profile. Table 2 presents the FA profile of CB, mango kernel fat-stearin (MKF-stearin) fraction, and RBO blends. Similar as previous studies by Jahurul et al. [9] and Biswas et al. [2], palmitic, stearic, and oleic acids are the major three FAs in CB (Table 3). RBO was rich in oleic and palmitic acids (42.87% and 21.05%, respectively), whereas MKF-stearin contained a higher amount of stearic acid followed by oleic acid and palmitic acid (58.57%, 22.12%, and 15.71%, respectively) (Table 2). Both were blended at various mass ratios as neither fat matched the FA composition of CB. While stearic acid content raised considerably ($p < 0.05$) with the increment of MKF-stearin content in the blends, oleic acid content declined significantly ($p < 0.05$) (Table 2). The percentage of palmitic acid content declined gradually with the addition of MKF-stearin. Among all the blends, blend G (60 : 40) showed similar stearic acid content and blend E (40 : 60) represented an analogous oleic acid content to CB. Previously, blends of supercritical carbon dioxide-extracted MKF and palm stearin were reported to have close FA profile to CB [9]. Blends (palm midfraction/palm stearin/olive oil blends and palm midfraction/palm stearin/refined bleached deodorized palm kernel oil) were also reported to show comparable FA profile as CB, with exception of the stearic acid content where the stearic acid content was lower in these blends. These blends were reported as the possible options to be used as CBS [2, 28]. In our study, three blends, blends E (40 : 60), F (50 : 50), and G (60 : 40), showed comparable percentages of oleic and stearic acid content and lower percentages of palmitic acid content compared to CB. In blend E (40 : 60), although the oleic acid content was similar to CB, it contained lower amount of stearic acid. Similarly, blend G (60 : 40) was sufficient with stearic acid, however lacking in oleic acid. In blend F (50 : 50), stearic and oleic acids were comparable with CB. Only palmitic acid was limited in blend F (50 : 50); therefore, the addition of palmitic acid in this blend can improve the chemical profile, which may help

Table 3: Analysis of variance (ANOVA) for response surface quadratic model.

Source	Sum of square	Degree of freedom	Mean square	F value	p value	Remarks
Model	68.19	9	7.58	10.57	<0.0001	Significant
A (time)	15.81	1	15.81	22.06	<0.0001	Significant
B (temperature)	8.01	1	8.01	11.18	0.0023	Significant
C (enzyme load)	10.76	1	10.76	15.02	0.0006	Significant
AB	0.2988	1	0.2988	0.4170	0.5235	
AC	4.61	1	4.61	6.43	0.0168	Significant
BC	0.0062	1	0.0062	0.0087	0.9263	
A^2	4.86	1	4.86	6.77	0.0144	Significant
B^2	3.17	1	3.17	4.42	0.0442	Significant
C^2	19.10	1	19.10	26.66	<0.0001	Significant
Residual	20.78	29	0.7167			
Lack of fit	16.55	19	0.8709	2.06	0.1215	Not significant
Pure error	4.24	10	0.4236			
Correlation total	89.09	39				

to mimic the FA profile of CB. Considering these factors, blend F (50 : 50) was chosen for further acidolysis reaction with the addition of palmitic acid in the presence of Lipozyme TL IM enzyme.

3.3. Enzymatic Acidolysis Reaction Model Development. The response variable (saturate–oleoyl–saturate; SOS) varied between 64.8% and 71.1%. Table 3 shows the analysis of variance for response surface quadratic model. After employing multiple regression analysis on the experimental data, the test and response variables were associated by the following polynomial equation:

$$Y = 67.25 + 0.76A - 0.54B + 0.62C + 0.14AB + 0.53AC - 0.2BC - 0.41A^2 + 0.33B^2 + 0.81C^2, \quad (1)$$

where Y is the SOS (saturate–oleoyl–saturate, %) and A, B, and C were representing the coded values for time (h), temperature (°C), and enzyme load (w/w), respectively.

The ANOVA of the quadratic regression model showed that the lack of fit was insignificant and the model p value ($p < 0.0001$) was significant. Along with this, the determination coefficient (R^2) was 0.766, and high degree of precision and reliability also confirmed with low level of coefficient of variation (CV% = 1.25).

The p value is a tool used to evaluate the significance of each coefficient, which in turn may disclose the pattern of the interactions between the variables. Based on the parameter optimization coefficient estimate, the independent variables (A, B, and C), three quadratic terms (A^2, B^2, and C^2), and cross product coefficient (AC) had a substantial contribution to the final product's SOS percentage. The outcome also demonstrated that reaction time, followed by temperature and enzyme load, had the greatest influence on SOS (Table 3).

Kadivar et al. [11] reported that water content, time, temperature, and enzyme load had significant impact on SOS yield to produce a cocoa butter equivalent from high oleic sunflower oil. Similarly, Biswas et al. [17] optimized time, temperature, and enzyme load to produce a cocoa butter substitute from a ternary palm oil blend with stearic and oleic acid.

3.4. Interactions between Parameters with Condition Optimization. The interaction between two different variables was shown in contour plots in Figure 1. The temperature (°C) was fixed at the center value, while the interaction between time (h) and enzyme load (w/w) was shown in Figure 1(a). From Figure 1(a), it was observed that the SOS percentages significantly ($p < 0.05$) increased with the increase of both time and enzyme load. The highest percentage of SOS was recorded with 8 h reaction time and 8% enzyme load. Figure 1(b) represents the interaction between time and temperature on SOS (%) while enzyme load (w/w) was fixed at its central value. This graph (Figure 1(b)) showed the highest level of SOS (%) at the longest amount of reaction time (8 h). On the other hand, SOS (%) did not increase significantly with the increment of temperature from 50°C to 70°C. At the highest temperature and the lowest time duration of reaction, the output was observed at the lowest. Interaction between temperature and enzyme load is presented in Figure 1(c) while time was constant at its central value. As it has been already shown in Figures 1(a) and 1(b), with temperature increment, SOS (%) did not increase whereas the opposite trend was observed for enzyme load. With the highest enzyme load and the lowest temperature, the SOS (%) was at its highest. As shown in Figure 1, the optimum reaction conditions were analyzed as 50°C, 8 h with 8% enzyme load. All the three parameters have a significant impact on SOS yield (Table 3). However, reaction time was the most significant parameter, affecting the highest percentages of SOS in the interesterification

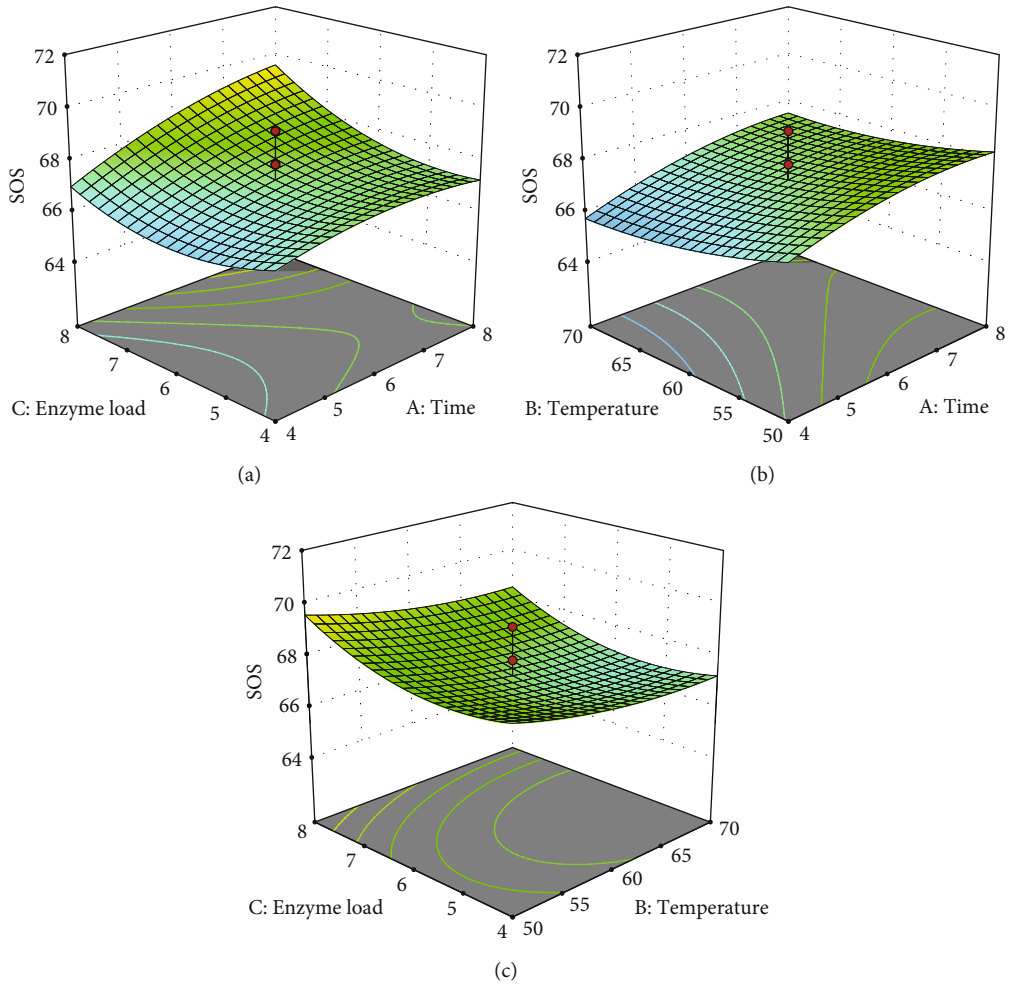

Figure 1: Contour plots of interactions between (a) time and enzyme load, (b) time and temperature, and (c) temperature and enzyme load on % SOS (saturate–oleoyl–saturate).

reaction. Previously, Kadivar et al. [11] reported reaction time, temperature, enzyme load, and water content to have significantly impacted SOS yield during the optimization and production of a cocoa butter equivalent. Mutia et al. [29] also reported substrate ratio, reaction time, and enzyme load to have a significant impact on the production of a cocoa butter equivalent. Similarly, reaction time, temperature, substrate ratio, water content, and pressure were optimized by Shekarchizadeh et al. [30] in the production of a cocoa butter analog using an algorithm.

3.5. Validation of the Model. RSM helps to save raw materials and time compared to traditional single parameter optimization [31]. To validate the model adequacy (Eq. (1)), a verification experiment was conducted under optimum reaction condition (reaction time 8 h, reaction temperature 50°C, and enzyme load (w/w) 8%). Table 4 shows the model verification conditions and SOS (%) for experimental and predicted values. A nonsignificant difference between the experimental and predicted values at the point of interest is needed to validate the model. The mean value of SOS (%) was 67.37 ± 0.43 (%) ($n = 3$) from the experimental data, which was close to predicted value (67.24). No significant difference was observed between experimental and predicted results which indicated validation of the RSM model. This also indicated that the adequacy was achieved for the expected optimization. This analysis revealed that the predicted and experimental values were in concord, and the model of Eq. (1) was accurate and satisfactory. After reaction condition optimization for acidolysis reaction and model validation of 50 : 50 blend with 10% palmitic acid, the saturate–oleoyl–saturate percentage in the final product was comparable to CB. Therefore, this final output product will be considered as CBA for further analysis in this study.

3.6. Free Fatty Acid Removal and Blending with CB. During the enzymatic interesterification reaction, lipases catalyze the hydrolysis of a broad range of oils to form diacylglycerols, monoacylglycerols, glycerol, and FFAs [32]. Therefore, FFA content becomes higher after the acidolysis reaction. Alkaline neutralization decreased the FFA content to 1.5% (data not presented), which aligns with the accepted range of FFA content in CB [33]. CB contains a FFA concentration of 1.1% (data not presented).

Table 4: TAG composition of MKF-stearin, RBO, their 50 : 50 blends, and CBA blends with CB in different ratios.

	POP	POSt	StOSt
CB	20.22 ± 0.21^{cde}	40.91 ± 0.30^{a}	26.48 ± 0.24^{a}
RBO	26.82 ± 0.06^{a}	0.70 ± 0.43^{j}	0.16 ± 0.28^{e}
MKF-stearin	14.75 ± 0.09^{f}	27.33 ± 1.08^{h}	20.33 ± 1.46^{cd}
50 : 50 blend	22.87 ± 0.05^{b}	10.5 ± 0.09^{i}	7.21 ± 0.27^{g}
5% CBA	20.05 ± 0.80^{de}	39.96 ± 0.53^{ab}	25.85 ± 0.16^{a}
10% CBA	20.17 ± 0.13^{de}	38.35 ± 0.27^{bc}	24.99 ± 0.37^{a}
20% CBA	20.48 ± 0.43^{cde}	37.30 ± 0.84^{cd}	23.22 ± 0.31^{b}
30% CBA	21.41 ± 0.12^{bcd}	36.15 ± 0.50^{d}	21.68 ± 0.39^{bc}
40% CBA	21.74 ± 0.09^{bcd}	34.25 ± 0.22^{e}	20.14 ± 0.23^{cd}
50% CBA	22.45 ± 0.31^{bc}	32.21 ± 0.24^{f}	19.83 ± 0.16^{d}
100% CBA	18.27 ± 0.57^{e}	30.31 ± 0.88^{g}	18.79 ± 0.13^{d}

[1]Each value represents mean ± standard deviation of the three replicates ($n = 3$). Different superscript letters in the same column represent significant statistical differences ($p < 0.05$). [2]CB = cocoa butter; RBO = rice bran oil; MKF-stearin = mango kernel fat-stearin; CBA = cocoa 3 butter alternative; P = palmitic acid; O = oleic acid; St = stearic acid.

3.7. Triacylglycerol Profile. The TAG profile is an important chemical property which influences the other physical properties of the fats and their blends. Table 4 shows the TAG composition of MKF-stearin, RBO, their 50 : 50 blends, and blends of CB and CBAs. The rearrangement of TAGs occurs after the acidolysis reactions in presence of Lipozyme TL IM enzyme in the oil blends and palmitic acid. CB contained a major portion of monounsaturated (SUS; S, saturated; U, unsaturated) TAGs (87.63% of POP, POSt, and StOSt), which was similar as previous literature [2, 5]. The remaining portion of TAGs was covered by other TAGs like diunsaturated, triunsaturated, or trisaturated ones. Before acidolysis reaction, RBO contained minimal StOSt content whereas MKF-stearin fraction showed higher content of StOSt compared to RBO. POP was significantly ($p < 0.05$) higher for RBO. After blending and acidolysis reaction with palmitic acid, the monounsaturated TAG content (67.37%) improved significantly ($p < 0.05$) compared to individual oils, and this content was comparable with CB. This outcome is akin to previous findings by Kadivar et al. [11] and Biswas et al. [17] where both of them utilized enzymatic acidolysis to produce CBE and CBS. After blending the CBA with CB at different ratios, the amount of POP, POSt, and StOSt decreased as the CBA blends increased. The percentage of POP did not vary significantly ($p < 0.05$) except at 100% CBA whereas StOSt varied significantly ($p < 0.05$) beyond 10% replacement. Up to 5 to 10% replacement of CB with CBAs, POP, and StOSt percentage did not vary significantly. The compositional variation of TAGs influences the crystal structures and melting profile of the CBA blends (Figures 2 and 3, respectively). The formation of β crystals depends on the StOSt content, while β' crystal formation relies on the POP/POSt content ratio [34].

3.8. Crystal Morphology. Crystal morphology is important as this is related to texture and mechanical properties of the final products [35]. Figure 2 represents the crystals of MKF-stearin, RBO, 50 : 50 blend, and CBA and CB blends. CB crystals were feather like spherulitic structures which looked like small flowers. RBO showed granular structure smaller than 20 μm in size whereas MKF-stearin crystals were spherulites in nature, demonstrating a smooth appearance with a size of 50-100 μm and connected in a network (Figure 2). After blending of RBO and MKKF-stearin, the crystal density for 50 : 50 oil blend was improved compared to RBO and the formation of crystal network was similar as MKF-stearin fraction.

After acidolysis reaction, the crystals appeared as both spherulite and granular in CBA; however, the network among all the crystals was not even observed for CB. In all the CBA-containing blends, granular structures were observed. The crystal network was finer and less spherulite compared to CB. These crystal structures, sizes, shapes, and polymorphs are important as they may have an influence on the texture characteristics of the final product [36]. Similar CB crystals were reported by Biswas et al. [17], Sonwai et al. [5], and Chen et al. [37]. Different composition of TAGs may have an influence on the crystal shapes in CB and CBA blends (Table 4). Different crystal morphologies mainly depend on the composition of TAGs as well as processing conditions. High-melting TAGs influence the formation of spherulite-like crystals whereas low-melting TAGs are related to the network formation and granular structures [38]. Chen et al. [37] reported that granular crystal was related to FFA content. In this study, CBA contained more FFA compared to CB (data not presented) which could be another possible reason of the presence of more granular crystals in CBAs.

3.9. Melting Profile. Melting thermograms are influenced by the TAG composition and SFC of the fat. The DSC melting profile of CB, MKF-stearin, RBO, 50 : 50 blend, and CBA and CB blends is presented in Figure 3. CB demonstrated a major endothermic peak at 20°C, whereas MKF-stearin melting peak was observed around 60°C and RBO started melting at very low temperature (below 0°C). The presence of different TAGs can be responsible for a high- or low-melting profile [39]. This low peak temperature can be explained by the minimal StOSt percentage in RBO (Table 4) and very low SFC content. Besides the StOSt content, other high-melting TAGs could possibly have been present in MKF-stearin. Those high-melting TAGs (possibly trisaturated) may cause the higher melting endotherms (Figure 3). Similarly, other low-melting TAGs (possibly triunsaturated) can affect the RBO endotherm. In the 50:50 oil blend ratio, both low- and high-melting peaks were observed (Figure 3). After acidolysis reaction and blending with CB, the change in melting curves was observed with the addition of CBA in CB (Figure 3). In the case of 100% CBA, one peak showed a similar pattern to CB with a less pronounced shape at 20°C and another broad high-melting peak at around 40°C. For 40% and 50% replacement of CBA in CB, some smaller and wider peaks were observed at higher temperatures along with the main peak. This could be due to the presence of high-melting TAGs (possibly trisaturates) in CBA, which leads to that high-melting peak. Up

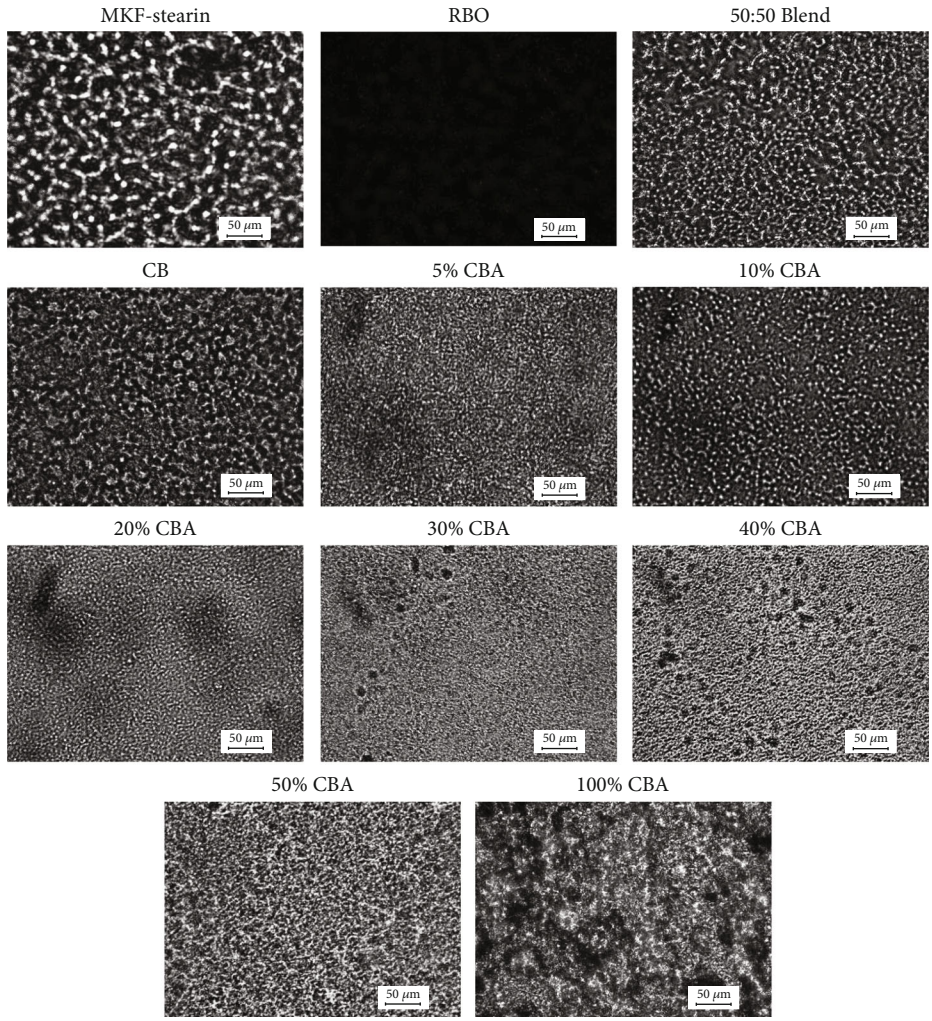

Figure 2: Crystal morphology of MKF-stearin, RBO, 50 : 50 oil blend, and CB and CBA blends. The white portion indicates the crystals, and the black areas represent the liquid phase.

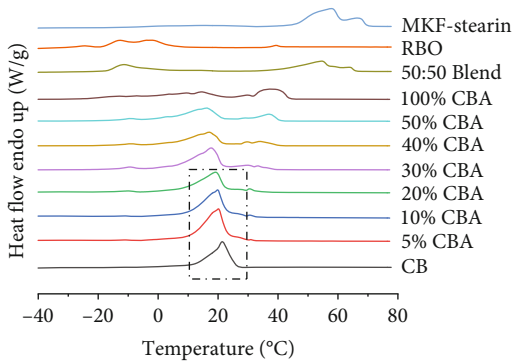

Figure 3: Melting profile of MKF-stearin, RBO, 50 : 50 blend, and CBA blends with CB. Box in dot-dashed lines indicates the major melting peaks of CBAs and CB.

to 20% CBA replacement, the single peak observed at 20°C was similar to CB (Figure 3). A similar pattern was observed for the melting profiles of CBE and CBS by Kadivar et al. [40] and Biswas et al. [17], respectively. Blends, which contain a higher amount of total monounsaturated TAG content, showed a single melting peak, similar to CB. There was no difference in the onset temperature with up to 20% addition.

3.10. Polymorphism Profile. Different polymorphs have different chain packing, sizes, and shapes, and they vary in their thermal stability and melting properties [41]. The hydrocarbon chain packing can be identified by XRD, which gives information about the short spacing on subcell structures [42]. In this study, polymorphic structures were studied by using XRD analysis for individual MKF-stearin and RBO, their 50 : 50 blend, and CB and CBA blends. Figure 4 represents the presence of various polymorphic forms in different oil blends and CB. CB demonstrated diffraction peaks at $d = 3.8 - 4.3$ Å (β' polymorph) and 4.5-4.6 Å (β polymorph), which is in agreement with previous literatures [17, 43, 44]. MKF-stearin exhibited similar β and β' crystals' peaks as CB where β' covered the major portion. RBO did not show any peak for β or β' crystals indicating that it is in amorphous

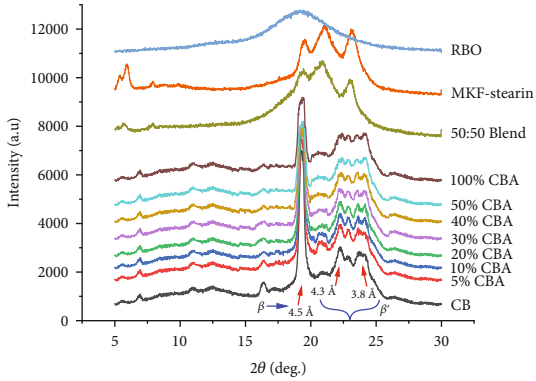

Figure 4: X-ray diffractograms of MKF-stearin, RBO, 50 : 50 blend, and CBA blends with CB (β' polymorph ($d = 3.8 - 4.3$ Å) and β polymorph ($d = 4.5 - 4.6$ Å)).

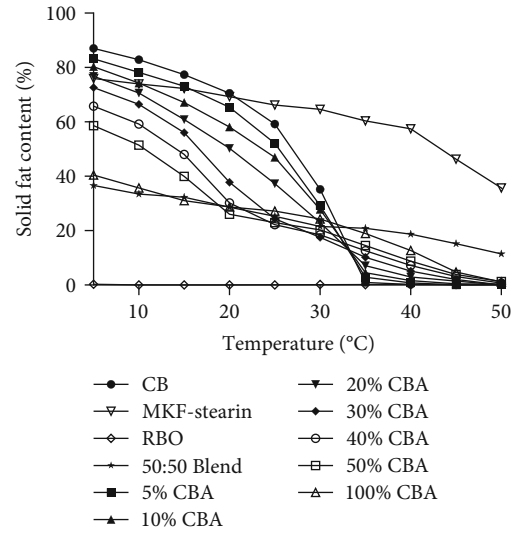

Figure 5: SFC analysis of MKF-stearin, RBO, 50 : 50 blend, and CBA and CB blends.

form. In the 50 : 50 oil blend, the intensity diffraction peaks were representing the presence of both β and β' crystals which were similar to that of MKF-stearin.

In the enzymatically produced CBA, the diffraction peak is shown at 4.5 and 3.8-4.3 Å. However, the intensity of the CBA peak at 4.5 Å, which was the β form of crystal, was lower compared to CB. With the increment of the CBA percentages in CB, the intensity for the prominent peaks at 4.5 Å, which is β form, was reducing. On the other hand, the intensity of peaks from 3.9 to 4.3 Å, which corresponded to β' form, increased. In the blends of 5 to 20% CBA, β form was observed along with the β' form. In the blends of 30-50% CBA, the β form slowly diminished with the progression of percentage of CBA, while β' polymorphs became the more prominent form. This difference could possibly be due to the lower amount POP, POSt, and StOSt TAGs in CBA and CB. Sato [39] reported that StOSt and POP TAGs can form stable β polymorph. In Table 4, it was observed that with the increase of CBA percentage in the blends, the percentages of POP and StOSt were decreasing. Therefore, these decreased percentages of POP and StOSt may negatively impact the formation of stable β crystals. This current study is in line with the previous studies on enzymatically produced CBAs [13, 17]. Podchong et al. [45] also reported β' as the prominent crystal polymorph for CBS as two strong spacings at 3.82 and 4.23 Å were reported.

3.11. Solid Fat Content. Solid fat content is a property which is related to the melting profile of fats. Figure 5 shows the SFC profile of MKF-stearin fraction, RBO, their 50 : 50 blend, and CB and CBA blends in different percentages. CB contained a higher percentage of SFC (>80%) than other blends until 20°C, proceeded by a sharp reduction to 35°C and complete melting at 40°C. This is consistent with previous reports by Biswas et al. [46] and Kadivar et al. [40]. SFC content of MKF-stearin was more than 70% whereas RBO showed a very minimum SFC content. Over the temperature progression, the SFC of MKF-stearin was higher compared to others. This could possibly be explained by their TAG profile. De Graef et al. [47] reported that β' polymorphs, formed from PPP (P, palmitic acid) and StStSt (St, stearic acid), melt at 53.57-56.60°C and 61.64-63.2°C, respectively. The presence of these trisaturates or other high-melting TAGs may influence the high SFC at higher temperature. After acidolysis reaction and replacement with CB, the SFC of CBA was comparable with CB up to 20% replacement. Up to 20% replacement, CBA and CB blends melted completely at body temperature and the SFC reduction was as sharp as CB.

All more than 20% CBA replacement blends needed higher temperature to melt completely. Sato [39] reported that trisaturates (SSS, S, saturated) melt at higher melting points at 55.0-73.0°C. In the previous studies, it was mentioned that confectionery fat should contain 63% SFC at 20°C, 40% at 25°C, and 0% at 37°C [48]. Biswas et al. [17] and Kadivar et al. [40] reported less than 40% SFC at 25°C for CBS and CBE in their studies. In our study, SFC was 32% at 25°C which was comparable with previous findings. It is desirable to melt completely at 37°C for confectionery fats; CBA replacement beyond 20% may not be useful in confectionery application. The higher SFC gives firmness to the fats that imparts rigidity and plasticity of the fat materials [49].

4. Conclusion

In this current study, optimum reaction condition for acidolysis reaction using oil blends was investigated for CBA production. The properties of CBA and CB blended with CBA were also analyzed. The optimum reaction condition for CBA production was 8% enzyme load (w/w), 8 h reaction time at 50°C with 250 rpm to produce maximum percentage of monounsaturated TAGs. After blending CBA with CB, polymorphism, melting profile, and SFC were similar up to 20% blending of CBA with CB. At lower blending up to 10% of CBA with CB, no significant differences were observed in terms of TAG profile. As CBR is compatible

with CB up to a certain percentage after which its TAG profile does not mimic that of CB, therefore, it is concluded that a replacement of up to 20% CBA can be used as a CBR. Since both oils in the blends are originated from by-products, using these two oils together may have an impact on waste minimization and contribute to a more sustainable food system in the confectionery industry.

Data Availability

The data that support the findings of this study are available from the corresponding author upon reasonable request.

Additional Points

Novelty Impact Statement. The current study examined the physicochemical properties of cocoa butter alternative (CBA) enzymatically produced from mango kernel fat-stearin and rice bran oil. The optimum reaction conditions for enzymatically produced CBA were 8 h, 8% enzyme load, and 50°C. Results demonstrated no significant differences in terms of polymorphism, melting profile, and solid fat content for up to 20% CBA replacement. Therefore, it can be used as cocoa butter replacer for up to 20% replacement in the confectionery industry.

Conflicts of Interest

The authors declared no conflict of interest.

Authors' Contributions

Mansura Mokbul was responsible for the conceptualization and formal analysis, investigation, methodology, software, validation, visualization, and original draft writing. Yuen Lin Cheow was responsible for the supervision, review, editing, and resources. Lee Fong Siow was responsible for the resources and funding, supervision, review, and editing.

Acknowledgments

The present work is funded by the graduate research grant of Monash University, Malaysia. Open Access publishing was facilitated by Monash University, as part of the Wiley - Monash University agreement via the Council of Australian University Librarians.

Supplementary Materials

Table S1 shows the factor variables and responses for optimization reaction conditions of SOS yield production. *(Supplementary Materials)*

References

[1] N. de Clercq, S. Kadivar, D. van de Walle, S. De Pelsmaeker, X. Ghellynck, and K. Dewettinck, "Functionality of cocoa butter equivalents in chocolate products," *European Food Research and Technology*, vol. 243, pp. 309–321, 2016.

[2] N. Biswas, Y. L. Cheow, C. P. Tan, and L. F. Siow, "Blending of palm mid-fraction, refined bleached deodorized palm kernel oil or palm stearin for cocoa butter alternative," *Journal of the American Oil Chemists' Society*, vol. 93, no. 10, pp. 1415–1427, 2016.

[3] M. Lipp and E. Anklam, "Review of cocoa butter and alternative fats for use in chocolate-part A. Compositional data," *Food Chemistry*, vol. 97, pp. 73–97, 1998.

[4] M. Mokbul, Y. L. Cheow, and L. F. Siow, "Physical properties, sensory profile and storage stability of compound chocolates made with cocoa butter replacer consisting of mango kernel fat and rice bran oil," *Food Chemistry Advances*, vol. 3, article 100515, 2023.

[5] S. Sonwai, P. Kaphueakngam, and A. Flood, "Blending of mango kernel fat and palm oil mid-fraction to obtain cocoa butter equivalent," *Journal of Food Science and Technology*, vol. 51, no. 10, pp. 2357–2369, 2014.

[6] M. H. A. Jahurul, I. S. M. Zaidul, N. A. N. Norulaini et al., "Cocoa butter fats and possibilities of substitution in food products concerning cocoa varieties, alternative sources, extraction methods, composition, and characteristics," *Journal of Food Engineering*, vol. 117, no. 4, pp. 467–476, 2013.

[7] J. Jin, P. Warda, H. Mu et al., "Characteristics of mango kernel fats extracted from 11 China-specific varieties and their typically fractionated fractions," *Journal of the American Oil Chemists' Society*, vol. 93, no. 8, pp. 1115–1125, 2016.

[8] S. P. Kochhar, "Minor and speciality oils," in *Vegetable Oils in Food Technology*, p. 291, Blackwell Publishing Ltd., 2011.

[9] M. H. A. Jahurul, I. S. M. Zaidul, N. A. Nik Norulaini et al., "Cocoa butter replacers from blends of mango seed fat extracted by supercritical carbon dioxide and palm stearin," *Food Research International*, vol. 65, pp. 401–406, 2014.

[10] J. J. Salas, M. A. Bootello, E. Martínez-Force, and R. Garcés, "Production of stearate-rich butters by solvent fractionation of high stearic–high oleic sunflower oil," *Food Chemistry*, vol. 124, no. 2, pp. 450–458, 2011.

[11] S. Kadivar, N. De Clercq, D. V. De Walle, and K. Dewettinck, "Optimisation of enzymatic synthesis of cocoa butter equivalent from high oleic sunflower oil," *Journal of the Science of Food and Agriculture*, vol. 94, no. 7, pp. 1325–1331, 2014.

[12] X. Xu, S. Balchen, C.-E. Høy, and J. Adler-Nissen, "Pilot batch production of specific-structured lipids by lipase-catalyzed interesterification: preliminary study on incorporation and acyl migration," *JAOCS*, vol. 75, no. 2, pp. 301–308, 1998.

[13] J. Jin, C. C. Akoh, Q. Jin, and X. Wang, "Preparation of mango kernel fat stearin-based hard chocolate fats via physical blending and enzymatic interesterification," *LWT*, vol. 97, pp. 308–316, 2018.

[14] H.-X. Wang, H. Wu, C.-T. Ho, and X.-C. Weng, "Cocoa butter equivalent from enzymatic interesterification of tea seed oil and fatty acid methyl esters," *Food Chemistry*, vol. 97, no. 4, pp. 661–665, 2006.

[15] I. O. Mohamed, "Lipase-catalyzed acidolysis of palm mid fraction oil with palmitic and stearic fatty acid mixture for production of cocoa butter equivalent," *Applied Biochemistry and Biotechnology*, vol. 171, no. 3, pp. 655–666, 2013.

[16] D. Undurraga, A. S. Markovits, and S. Erazo, "Cocoa butter equivalent through enzymic interesterification of palm oil midfraction," *Process Biochemistry*, vol. 36, no. 10, pp. 933–939, 2001.

[17] N. Biswas, Y. L. Cheow, C. P. Tan, and L. F. Siow, "Physicochemical properties of enzymatically produced palm-oil-based cocoa butter substitute (CBS) with cocoa butter mixture," *European Journal of Lipid Science and Technology*, vol. 120, no. 3, 2018.

[18] S. Soekopitojo, P. Hariyadi, T. R. Muchtadi, and N. Andarwulan, "Enzymatic interestrification of palm oil mid fraction blend for production of cocoa butter equivalent," *Asian Journal of Food and Agro-Industry*, vol. 2, pp. 807–816, 2009.

[19] A. Y. Aydar, "Utilization of Response Surface Methodology in Optimization of Extraction of Plant Materials," in *Statistical Approaches With Emphasis on Design of Experiments Applied to Chemical Processes*, pp. 157–169, InTech, 2018.

[20] M. Friedman, "Rice brans, rice bran oils, and rice hulls: composition, food and industrial uses, and bioactivities in humans, animals, and cells," *Journal of Agricultural and Food Chemistry*, vol. 61, no. 45, pp. 10626–10641, 2013.

[21] N. Nantiyakul, S. Furse, I. Fisk, T. J. Foster, G. TuckeR, and D. A. Gray, "Phytochemical composition of Oryza sativa (rice) bran oil bodies in crude and purified isolates," *Journal of the American Oil Chemists' Society*, vol. 89, no. 10, pp. 1867–1872, 2012.

[22] N. Pengkumsri, C. Chaiyasut, B. S. Sivamaruthi et al., "The influence of extraction methods on composition and antioxidant properties of rice bran oil," *Food Science and Technology*, vol. 35, no. 3, pp. 493–501, 2015.

[23] E. Momeny, N. Vafaei, and N. Ramli, "Physicochemical properties and antioxidant activity of a synthetic cocoa butter equivalent obtained through modification of mango seed oil," *International Journal of Food Science & Technology*, vol. 48, no. 7, pp. 1549–1555, 2013.

[24] FAO, *FAOSTAT*, FAO, 2022, [Accessed 05/01/2023 2023], https://www.fao.org/statistics/en.

[25] J. Jin, H. Mu, Y. Wang et al., "Production of high-melting symmetrical monounsaturated triacylglycerol-rich fats from mango kernel fat by acetone fractionation," *Journal of the American Oil Chemists' Society*, vol. 94, no. 2, pp. 201–213, 2017.

[26] S. S. Narine and A. G. Marangoni, "The difference between cocoa butter and Salatrim® lies in the microstructure of the fat crystal network," *Journal of American Oil Chemists' Society*, vol. 76, no. 1, pp. 7–13, 1999.

[27] European Parlament and Council, *Directive 2000/36/EC of the European Parliament and of the council of 23 June 2000 Relating to Cocoa and Chocolate Products Intended for Human Consumption*, pp. 19–25, European Union Directive, 2000.

[28] F. Hashempour-Baltork, M. Torbati, S. Azadmard-Damirchi, and G. P. Savage, "Vegetable oil blending: a review of physicochemical, nutritional and health effects," *Trends in Food Science & Technology*, vol. 57, pp. 52–58, 2016.

[29] R. Mutia, D. N. Abang Zaidel, and I. I. Muhamad, "Optimization of cocoa butter equivalent production from formulated hard palm oil mid-fraction and canola oil blends," *Jurnal Teknologi*, vol. 78, no. 6-12, 2016.

[30] H. Shekarchizadeh, R. Tikani, and M. Kadivar, "Optimization of cocoa butter analog synthesis variables using neural networks and genetic algorithm," *Journal of Food Science and Technology*, vol. 51, no. 9, pp. 2099–2105, 2014.

[31] V. Samavati, "Polysaccharide extraction from Abelmoschus esculentus: optimization by response surface methodology," *Carbohydrate Polymers*, vol. 95, no. 1, pp. 588–597, 2013.

[32] S. Sivakanthan and T. Madhujith, "Current trends in applications of enzymatic interesterification of fats and oils: a review," *LWT*, vol. 132, article 109880, 2020.

[33] O.-W. Achaw, E. Danso-Boateng, O. W. Achaw, and E. Danso-Boateng, "Cocoa processing and chocolate manufacture," in *Chemical and Process Industries*, O.-W. Achaw and E. Danso-Boateng, Eds., Springer, Cham, 2021.

[34] J. F. Toro-Vazquez, D. Pérez-Martínez, E. Dibildox-Alvarado, M. Charó-Alonso, and J. Reyes-Hernández, "Rheometry and polymorphism of cocoa butter during crystallization under static and stirring conditions," *Journal of the American Oil Chemists' Society*, vol. 81, no. 2, pp. 195–202, 2004.

[35] N. C. Acevedo and A. G. Marangoni, "Nanostructured fat crystal systems," *Annual Review of Food Science and Technology*, vol. 6, no. 1, pp. 71–96, 2015.

[36] O. N. Çiftçi, S. Fadıloğlu, and F. Göğüş, "Conversion of olive pomace oil to cocoa butter-like fat in a packed-bed enzyme reactor," *Bioresource Technology*, vol. 100, no. 1, pp. 324–329, 2009.

[37] J. Chen, S. M. Ghazani, J. A. Stobbs, and A. G. Marangoni, "Tempering of cocoa butter and chocolate using minor lipidic components," *Nature Communications*, vol. 12, no. 1, p. 5018, 2021.

[38] Y. Shi, B. Liang, and R. W. Hartel, "Crystal morphology, microstructure, and textural properties of model lipid systems," *Journal of the American Oil Chemists' Society*, vol. 82, no. 6, pp. 399–408, 2005.

[39] K. Sato, "Molecular aspects in fat polymorphism," in *Crystallization and Solidification Properties of Lipids*, E. A. Neil Widlak, Ed., pp. 1–6, AOCS Press, 2001.

[40] S. Kadivar, N. De Clercq, M. Mokbul, and K. Dewettinck, "Influence of enzymatically produced sunflower oil based cocoa butter equivalents on the phase behavior of cocoa butter and quality of dark chocolate," *LWT-Food Science and Technology*, vol. 66, pp. 48–55, 2016.

[41] V. D'souza, J. M. Deman, and L. Deman, "Short spacings and polymorphic forms of natural and commercial solid fats: a review," *JAOCS*, vol. 67, no. 11, pp. 835–843, 1990.

[42] X. Zhang, L. Li, H. Xie et al., "Effect of temperature on the crystalline form and fat crystal network of two model palm oil-based shortenings during storage," *Food and Bioprocess Technology*, vol. 7, no. 3, pp. 887–900, 2014.

[43] S. Kadivar, N. De Clercq, S. Danthine, and K. Dewettinck, "Crystallization and polymorphic behavior of enzymatically produced sunflower oil based cocoa butter equivalents," *European Journal of Lipid Science and Technology*, vol. 118, no. 10, pp. 1521–1538, 2016.

[44] S. Sonwai and P. Ponprachanuvut, "Studies of fatty acid composition, physicochemical and thermal properties, and crystallization behavior of mango kernel fats from various Thai varieties," *Journal of Oleo Science*, vol. 63, no. 7, pp. 661–669, 2014.

[45] P. Podchong, P. Inbumrung, and S. Sonwai, "The effect of hard lauric fats on the crystallization behavior of cocoa butter substitute," *Journal of Oleo Science*, vol. 69, no. 7, pp. 659–670, 2020.

[46] N. Biswas, Y. L. Cheow, C. P. Tan, S. Kanagaratnam, and L. F. Siow, "Cocoa butter substitute (CBS) produced from palm mid-fraction/palm kernel oil/palm stearin for confectionery fillings," *Journal of the American Oil Chemists' Society*, vol. 94, no. 2, pp. 235–245, 2017.

[47] V. De Graef, J. Vereecken, K. W. Smith, K. Bhaggan, and K. Dewettinck, "Effect of TAG composition on the solid fat content profile, microstructure, and hardness of model fat blends with identical saturated fatty acid content," *European Journal of Lipid Science and Technology*, vol. 114, no. 5, pp. 592–601, 2012.

[48] R. E. Timms, "Physical properties of oils and mixtures of oils," *Journal of the American Oil Chemists' Society*, vol. 62, no. 2, pp. 241–249, 1985.

[49] J. M. N. Marikkar, H. M. Ghazali, and K. Long, "Composition and thermal characteristics of Madhuca longifolia seed fat and its solid and liquid fractions," *Journal of Oleo Science*, vol. 59, no. 1, pp. 7–14, 2010.